Supporting information

Determination of thermal properties of grouting materials for borehole heat exchangers (BHE)

Anna Albers[1*], *Petra Huttenloch*[2], *Roman Zorn*[2], *Hagen Steger*[1], *Philipp Blum*[1]

[1] Karlsruhe Institute of Technology (KIT), Institute of Applied Geosciences (AGW)

Kaiserstraße 12, 76131 Karlsruhe, Germany

[2] European Institute for Energy Research (EIFER), Emmy-Noether-Straße 11, 76131 Karlsruhe, Germany

*Corresponding author: anna.albers@kit.edu (+49 721 608 45064)

1. Literature review

Table A- 1: Measurement methods applied for the determination of thermal conductivity λ of grouting materials

Method		Literature	Specifications
Steady state		Alrtimi et al. (2013)	Own setup, source between two samples, saturated and dry samples
		Delaleux et al. (2012)	No information on the manufacturer (own setup?), Fourier's gradient, saturated sample
		Extremera-Jiménez et al. (2021)	Guarded heat flow meter FOX-50 (TA Instruments), ISO 8302
		Jobmann and Buntebarth (2009)	No information on the manufacturer (own setup?), divided bar
		Song et al. (2019)	TC3200 Thermal Conductivity Instrument, 3 – 5 % error, (probably) dry samples
		(Wang et al. 2020)	Guarded hot plate, TPMBE-300 thermal conductivity meter
Transient hot wire	Needle probe	Blázquez et al. (2017)	KD2-PRO analyzer, needle probe, sensor RK-1, Decagon devices
		Do et al. (2018); Do et al. (2017)	Own setup, needle probe, ASTM D5334, (partly) saturated samples
		Erol and François (2014); Erol and François (2013)	Hukseflux company, needle probe TP02, (partly) saturated
		Kim et al. (2017); Kim and Oh (2019)	KD2 PRO (Decagon Manufacturing Co., Ltd., Pullman, WA, USA), TR-1 (single needle), SH-1 (dual needle), 10 % accuracy, improved contact with grease, saturated and dry samples
		Dinh et al. (2020); Kim et al. (2020)	Own setup, ASTM D5334, (partly) saturated samples
		Li et al. (2019)	Needle probe: K-type thermocouple (WRN-130, ZUHUJIANG, China), own setup
		Indacoechea-Vega et al. (2018); Pascual-Muñoz et al. (2018)	Hukseflux TPSYS02, ASTM 5334-08, saturated samples
		Shafigh et al. (2020)	KD2-PRO analyser using a TR1 needle
	Surface probe	Allan (1997)	Shotherm QTM-D2 Thermal Conductivity Meter, surface probe, saturated samples
		Frąc et al. (2021)	Isomet 2104, surface probe, saturated and dry samples
		Kim et al. (2016); Kim et al. (2015); Kim and Oh (2020)	Quick Thermal Conductivity Meter QTM500, Kyoto Electronics Manufacturing Co.), PD-11 surface probe, 3 % reproducibility, 5 % accuracy, saturated and dry samples
		Lee et al. (2010); Park et al. (2011)	QTM-500 thermal conductivity meter (Kyoto Electronics), PD-12 probe, 3 % reproducibility, saturated samples
		Riegger et al. (2016)	Isomet 2104, surface probe, saturated samples
		Viccaro (2018)	Heat Flow Meter Shotherm QTM Showa Denko, 2 % reproducibility, UNI EN 12664:2002
Transient plane source		Bentz (2007)	HotDisk Thermal Constants Analyser, 2 % reproducibility, (partly) saturated samples
		Berktas et al. (2020)	HotDisk Thermal Constants Analyser, TPS 2500S, (partly) saturated samples
		Borinaga-Treviño et al. (2013)	TCi C-Therm thermal conductivity tester, improved contact with measurement oil, dry samples
		Delaleux et al. (2012)	No information on the manufacturer (own setup?), (partly) saturated samples
		Dong et al. (2022)	Unsteady thermal conductivity tester, Harbin Institute of Technology
		Yang et al. (2024)	DRE-2C type thermal conductivity tester, 5 % accuracy
		Zhao et al. (2024)	TPS instrument (TPS 500)
		Zhou et al. (2018)	Thermal Conductivity Meter (TCi)

Table A- 2: Measurement methods applied for the determination of specific heat capacity c_p and volumetric heat capacity ρc_p of grouting materials and other cementitious materials

Method	**Literature**	**Specifications**
Transient hot wire	Frąc et al. (2021)	Isomet 2104, surface probe, saturated and dry samples, measurement of the volumetric heat capacity
	Kim et al. (2017); Kim and Oh (2019)	KD2 PRO (Decagon Manufacturing Co., Ltd., Pullman, WA, USA), SH-1 (dual needle), 10 % accuracy, improved contact with grease, saturated and dry samples, measurement of ρc_p and thermal diffusivity α
Transient plane source	Bentz (2007)	HotDisk, c_p-module with gold cell, (partly) saturated sample
	Zhou et al. (2018)	Thermal Conductivity Meter (TCi), measurement of ρc_p
Calorimetry	Extremera-Jiménez et al. (2021)	ASTM D4611, dry sample, law of mixtures
	Liu et al. (2022)	DSC, Q2000, TA Instruments, USA, functional cement paste for geothermal-coal synergetic mining, heat range: 20-80 °C
	Schutter and Taerwe (1995)	DSC, hardening cement paste
	Shafigh et al. (2020)	DSC, law of mixtures, (sand, cement for the application as building material, dry samples, 20-50 °C)
	Xu and Chung (2000)	DSC, Perkin-Elmer Differential Scanning Calorimeter (Norwalk, CT, USA) (DSC-7), (cement-sand-mixtures for the application as building material)

Table A- 3: Sample preparation procedures applied for the analysis of thermal conductivity λ and volumetric heat capacity ρc_p of grouting materials

	Literature	Mixing device	Mixing routine
Mixing method	Allan (1997)	Dependent on sample size: capacity blender, Hobart planetary mixer (1 L); air-driven grout paddle mixer, ChemGrout CG- 55OP (129 L); air-driven colloidal grout mixer, ChemGrout CG620 (227 L)	5 min (with paddle mixer); 30-60 s (colloidal grout mixer)
	Bentz (2007)	High-speed blender	Several minutes and temperature-controlled
	Berktas et al. (2020)	High-share dispersion system from VMA Getzmann	No information provided
	Dong et al. (2022)	No information provided	Mix and stir for 10 min
	Frąc et al. (2021)	No information provided	PN-EN 196-1:2006, 120 s
	Indacoechea-Vega et al. (2018)	750 W mortar mixer with variable speed	No information provided
	Mascarin et al. (2022)	IKA mixer	2 steps of about 1.5 min, EN 196–1, increasing rotation speed up to 385 rpm, then manually remixing with a rubber spatula, at T = 20 °C, 65 % RH
	Mendes et al. (2019)	Mortar mixer	1 min low speed, 30 s high speed
	Pascual-Muñoz et al. (2018)	1500 W mortar mixer	Speed regulation
	Song et al. (2019)	No information provided	Starting at a low speed of 4000 ± 200 rpm, cement was added in 15 s, rotated at a high speed of 12 000 ± 500 rpm for 35 s
	Viccaro (2018)	Colloidal grout mixer	UNI EN 196-1:2016
	Xu and Chung (2000)	Rotary mixer with a flat beater	No further information ("all ingredients were mixed")
	Zhao et al. (2024)	High-speed hand mixer	at 600 rpm
	Literature	**Curing condition**	**Hydration time**
Curing conditions	Allan (1997)	Samples sealed to prevent evaporation, demoulded after 24 h, placed in a water bath	14 d
	Alrtimi et al. (2013)	No information provided	>14 d
	Bentz (2007)	Saturated (small volume of distilled water on top) or sealed conditions, at 20 °C	8 h, 1-2-3-8-15-28 d
	Berktas et al. (2020)	In climate chamber at 100 % RH and 20 °C	7 d
	Blázquez et al. (2017)	Dry (?) and harden	28 d
	Borinaga-Treviño et al. (2013)	At ambient temperature for 24 h – 2 d, demolition of moulds, submerged in water at 20 °C	14 d
	Dong et al. (2022)	Remove mould aft 24 h, cure in water	28 d
	Erol and François (2014)	80 % RH, at 20 °C	10 d and 30 d
	Frąc et al. (2021)	24 h in moulds, then immerse in water at 22 °C	28 d
	Indacoechea-Vega et al. (2018); Pascual-Muñoz et al. (2018)	48 h at ambient conditions, removal of moulds, immersed in water at 20 °C	28 d
	Kim et al. (2017); Kim et al. (2016); Kim and Oh (2020)	Ambient conditions, dried in the oven, saturated by placing in water for 2-5 d	28 d
	Mendes et al. (2019)	Demoulded after 24 h, in a moist chamber at 25 °C and 90 % RH	28 d

	Park et al. (2011)	Wet conditions	continuously for 14 d
	Riegger et al. (2016)	100 % RH, ambient conditions	7, 14, 21, 28 d
	Shafigh et al. (2020)	Removed from moulds after 24 h, in normal water at 23 °C	28 d
	Song et al. (2019)	In 8040D10 HTHP consistometer (Chandler Engineering Company, L.L.C) for 8 h, at T = 60 °C, p = 20 MPa	No information provided (> 8 h)
	Viccaro (2018)	Drying (?) at 20 °C, 95 – 99 % relative humidity	28 d
	Xu and Chung (2000)	Demoulding after 24 h, in the air at room temperature and 100 % RH	28 d
	Zhao et al. (2024)	Demould after 1 day, cure in lab environment at 23 ± 2 °C, 45 ± 10 % RH	28 d

2. Overview of the applied analyses

Table A- 4: List of the applied methods and the corresponding sample conditions (hydration time *t*, water content *w*, saturation S_r)

Material	Conditions					Applied methods		
	Mixing speed [rpm]	Curing condition	*t* [d]	*w* [%]	S_r [%]	Thermal conductivity	Specific heat capacity	Volumetric heat capacity
Measurement method								
M1	2000	Under water	28	73.0	101	THW, TPS	DSC	THW, TPS, DSC + calculation
M2	2000	Under water	28	69.8	102	THW, TPS	DSC	THW, TPS, DSC + calculation
M3	2000	Under water	28	29.2	100	THW, TPS	DSC	THW, TPS, DSC + calculation
M4	2000	Under water	28	58.3	99	THW, TPS	DSC	THW, TPS, DSC + calculation
M5	2000	Under water	28	30.8	99	THW, TPS	DSC	THW, TPS, DSC + calculation
M6	2000	Under water	28	52.9	101	THW, TPS	DSC	THW, TPS, DSC + calculation
M7	2000	Under water	28	39.1	101	THW, TPS	DSC	THW, TPS, DSC + calculation
Mixing speed								
M1	650	Under water	28	72.0	100	TPS	DSC	DSC + calculation
M2	650	Under water	28	71.9	100	TPS	DSC	DSC + calculation
M3	650	Under water	28	29.7	99	TPS	DSC	DSC + calculation
M5	650	Under water	28	32.2	100	TPS	DSC	DSC + calculation
Curing conditions								
M1	2000	Air-moist	28	70.2	98	TPS	DSC	DSC + calculation
M2	2000	Air-moist	28	69.2	99	TPS	DSC	DSC + calculation
M3	2000	Air-moist	28	26.4	94	TPS	DSC	DSC + calculation
M4	2000	Air-moist	28	55.3	-	TPS	DSC	-
M5	2000	Air-moist	28	30.1	102	TPS	DSC	DSC + calculation
Hydration time								
M1	2000	Under water	9	-	-	TPS	-	-
M1	2000	Under water	14	71.9	-	TPS	DSC	-
M1	2000	Under water	21	70.9	-	TPS	-	-
M1	2000	Under water	28	71.4	-	TPS	DSC	-
M1	2000	Under water	56	71.4	-	TPS	DSC	-
M1	2000	Under water	112	73.5	102	TPS	DSC	DSC + calculation
M1	2000	Under water	182	-	-	TPS	DSC	-
M1	2000	Under water	273	73.8	-	TPS	DSC	-
M1	2000	Under water	365	73.0	103	TPS	DSC	DSC + calculation
M2	2000	Under water	9	-	-	TPS	-	-
M2	2000	Under water	14	73.1	-	TPS	DSC	-
M2	2000	Under water	21	72.7	-	TPS	-	-
M2	2000	Under water	28	73.7	-	TPS	DSC	-
M2	2000	Under water	56	73.8	-	TPS	DSC	-
M2	2000	Under water	112	69.7	100	TPS	DSC	DSC + calculation
M2	2000	Under water	182	-	-	TPS	DSC	DSC + calculation

M2	2000	Under water	273	73.3	-	TPS	DSC	-
M2	2000	Under water	365	72.3	100	TPS	DSC	DSC + calculation
M3	2000	Under water	7	-	-	TPS	-	-
M3	2000	Under water	14	-	-	TPS	DSC	-
M3	2000	Under water	21	-	-	TPS	-	-
M3	2000	Under water	28	26.4	94	TPS	DSC	DSC + calculation
M3	2000	Under water	56	28.8	-	TPS	DSC	-
M3	2000	Under water	112	29.0	-	-	DSC	-
M3	2000	Under water	182	28.3	98	-	DSC	DSC + calculation
M3	2000	Under water	272	29.2	-	-	DSC	-
M3	2000	Under water	365	29.4	-	-	DSC	-
M4	2000	Under water	9	-	-	TPS	-	-
M4	2000	Under water	14	57.6	-	TPS	DSC	-
M4	2000	Under water	21	58.5	-	TPS	-	-
M4	2000	Under water	28	55.3	-	TPS	DSC	-
M4	2000	Under water	56	56.3	-	TPS	DSC	-
M4	2000	Under water	112	57.8	101	TPS	DSC	DSC + calculation
M4	2000	Under water	182	-	-	TPS	DSC	-
M4	2000	Under water	273	57.9	-	TPS	DSC	-
M4	2000	Under water	365	57.7	102	TPS	DSC	DSC + calculation

Transient hot wire (THW), transient plane source (TPS), differential scanning calorimetry (DSC)

3. Measurement uncertainties

Table A- 5: Determination of measurement uncertainties based on the recommendations of the *Guide to the Expression of Uncertainty in Measurement* (ISO IEC 98-3 2008).

Property	**Method**	**Uncertainty type A**	**Uncertainty type B**
Density of suspension	Mud balance	Reading accuracy [1] 0.01 g cm^{-1}	Single measurement
Wet bulk density	Immersion weighing	Accuracy of balance [2] 0.001 g	Standard deviation, incl. Student-t (2-3 measurements)
Water content	Gravimetry	Accuracy of balance [2] 0.001 g	Standard deviation, incl. Student-t (2-3 measurements)
Thermal conductivity	THW	Accuracy [3] 10 %	Standard deviation, incl. Student-t (4-8 measurements)
Thermal conductivity	TPS	Accuracy [4] 2 %	Standard deviation, incl. Student-t (3-5 measurements)
Volumetric heat capacity	THW	Accuracy [3] 15 % + 0.001 MJ m^{-3} K^{-1}	Standard deviation, incl. Student-t (4-8 measurements)
Volumetric heat capacity	TPS	Accuracy [4] 7 %	Standard deviation, incl. Student-t (3-5 measurements)
Specific heat capacity (dry samples, $c_{p,d}$)	DSC	Calibration [5] 1.5 % Integration, baseline [5] 3 % Mass of sample [6] 0.1 % Thermal contact [5] 0.2 %	Standard deviation, incl. Student-t (5 measurements)
Specific heat capacity (wet samples, $c_{p,f}$)	DSC, Water content	Equation 4	
Volumetric heat capacity	DSC, Water content, Wet bulk density	Equation 6	

[1] own estimate, [2] manufacturer value (Denver SI603, Sartorius AG, Germany), [3] manufacturer value (ISOMET 2104, Applied Precision Ltd., Slovakia), [4] manufacturer value (HotDisk TPS1500, C3 Prozess- und Analysentechnik, Germany), [5] Mettler Toledo (2016), [6] manufacturer value (Cubis II MCE 125P, Sartorius AG, Germany)

4. Differential scanning calorimetry

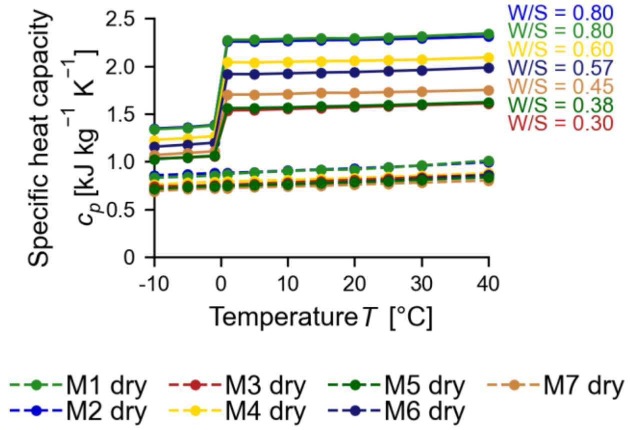

Fig. A- 1: Temperature dependence of the specific heat capacity using the differential scanning calorimetry (DSC) method. Sample preparation: Mixed at 2000 rpm, cured under water and hydration time of 28 days.

References

Allan, M.: Thermal conductivity of cementitious grouts for geothermal heat pumps, FY Progress Report. BNL 65129. New York: Brookhaven National Laboratory. (1997)

Alrtimi, A.A., Rouainia, M., Manning, D.A.C.: Thermal enhancement of PFA-based grout for geothermal heat exchangers. Applied Thermal Engineering. 54, 559–564 (2013). https://doi.org/10.1016/j.applthermaleng.2013.02.011

Bentz, D.P.: Transient plane source measurements of the thermal properties of hydrating cement pastes. Mater Struct. 40, 1073–1080 (2007). https://doi.org/10.1617/s11527-006-9206-9

Berktas, I., Nejad Ghafar, A., Fontana, P., Caputcu, A., Menceloglu, Y., Saner Okan, B.: Synergistic Effect of Expanded Graphite-Silane Functionalized Silica as a Hybrid Additive in Improving the Thermal Conductivity of Cementitious Grouts with Controllable Water Uptake. Energies. 13, 3561 (2020). https://doi.org/10.3390/en13143561

Blázquez, C.S., Martín, A.F., Nieto, I.M., García, P.C., Sánchez Pérez, L.S., González-Aguilera, D.: Analysis and study of different grouting materials in vertical geothermal closed-loop systems. Renewable Energy. 114, 1189–1200 (2017). https://doi.org/10.1016/j.renene.2017.08.011

Borinaga-Treviño, R., Pascual-Muñoz, P., Castro-Fresno, D., Del Coz-Díaz, J.J.: Study of different grouting materials used in vertical geothermal closed-loop heat exchangers. Applied Thermal Engineering. 50, 159–167 (2013). https://doi.org/10.1016/j.applthermaleng.2012.05.029

Delaleux, F., Py, X., Olives, R., Dominguez, A.: Enhancement of geothermal borehole heat exchangers performances by improvement of bentonite grouts conductivity. Applied Thermal Engineering. 33–34, 92–99 (2012). https://doi.org/10.1016/j.applthermaleng.2011.09.017

Dinh, B.H., Kim, Y., Kang, G.: Thermal conductivity of steelmaking slag-based controlled low-strength materials over entire range of degree of saturation: A study for ground source heat pump systems. Geothermics. 88, 101910 (2020). https://doi.org/10.1016/j.geothermics.2020.101910

Do, T.M., Kang, G., Kim, Y.: Thermal conductivity of controlled low strength material (CLSM) under various degrees of saturation using a modified pressure plate extractor apparatus – A case study for geothermal systems. Applied Thermal Engineering. 143, 607–613 (2018). https://doi.org/10.1016/j.applthermaleng.2018.07.116

Do, T.M., Kim, Y., Dang, M.Q.: Influence of curing conditions on engineering properties of controlled low strength material made with cementless binder. KSCE J Civ Eng. 21, 1774–1782 (2017). https://doi.org/10.1007/s12205-016-0731-y

Dong, S., Liu, G., Zhan, T., Yao, Y., Ni, L.: Performance study of cement-based grouts based on testing and thermal conductivity modeling for ground-source heat pumps. Energy and Buildings. 272, 112351 (2022). https://doi.org/10.1016/j.enbuild.2022.112351

Erol, S., François, B.: Thermal, hydraulic and mechanical performances of enhanced grouting materials for borehole heat exchanger. In: Musso, G. (ed.) Coupled Phenomena in Environmental Geotechnics. pp. 491–499. CRC Press (2013)

Erol, S., François, B.: Efficiency of various grouting materials for borehole heat exchangers. Applied Thermal Engineering. 70, 788–799 (2014). https://doi.org/10.1016/j.applthermaleng.2014.05.034

Extremera-Jiménez, A.J., Eliche-Quesada, D., Guitérrez-Montes, C., Cruz-Peragón1, F.: Experimental work over borehole filling material to reinforce characterization and model validation of Ground Heat Exchangers. REPQJ. 19, 109–114 (2021). https://doi.org/10.24084/repqj19.227

Frąc, M., Szudek, W., Szołdra, P., Pichór, W.: Grouts with highly thermally conductive binder for low-temperature geothermal applications. Construction and Building Materials. 295, 123680 (2021). https://doi.org/10.1016/j.conbuildmat.2021.123680

Indacoechea-Vega, I., Pascual-Muñoz, P., Castro-Fresno, D., Zamora-Barraza, D.: Durability of geothermal grouting materials considering extreme loads. Construction and Building Materials. 162, 732–739 (2018). https://doi.org/10.1016/j.conbuildmat.2017.12.072

ISO IEC 98-3: Uncertainty of measurement — Part 3: Guide to the expression of uncertainty in measurement (GUM:1995), (2008)

Jobmann, M., Buntebarth, G.: Influence of graphite and quartz addition on the thermo–physical properties of bentonite for sealing heat-generating radioactive waste. Applied Clay Science. 44, 206–210 (2009). https://doi.org/10.1016/j.clay.2009.01.016

Kim, D., Kim, G., Baek, H.: Relationship between thermal conductivity and soil–water characteristic curve of pure bentonite-based grout. International Journal of Heat and Mass Transfer. 84, 1049–1055 (2015). https://doi.org/10.1016/j.ijheatmasstransfer.2015.01.091

Kim, D., Kim, G., Baek, H.: Thermal conductivities under unsaturated condition and mechanical properties of cement-based grout for vertical ground-heat exchangers in Korea—A case study. Energy and Buildings. 122, 34–41 (2016). https://doi.org/10.1016/j.enbuild.2016.02.047

Kim, D., Kim, G., Kim, D., Baek, H.: Experimental and numerical investigation of thermal properties of cement-based grouts used for vertical ground heat exchanger. Renewable Energy. 112, 260–267 (2017). https://doi.org/10.1016/j.renene.2017.05.045

Kim, D., Oh, S.: Relationship between the thermal properties and degree of saturation of cementitious grouts used in vertical borehole heat exchangers. Energy and Buildings. 201, 1–9 (2019). https://doi.org/10.1016/j.enbuild.2019.07.017

Kim, D., Oh, S.: Measurement and comparison of thermal conductivity of porous materials using box, dual-needle, and single-needle probe methods-A case study. International Communications in Heat and Mass Transfer. 118, 104815 (2020). https://doi.org/10.1016/j.icheatmasstransfer.2020.104815

Kim, Y., Dinh, B.H., Do, T.M., Kang, G.: Development of thermally enhanced controlled low-strength material incorporating different types of steel-making slag for ground-source heat pump system. Renewable Energy. 150, 116–127 (2020). https://doi.org/10.1016/j.renene.2019.12.129

Lee, C., Lee, K., Choi, H., Choi, H.-P.: Characteristics of thermally-enhanced bentonite grouts for geothermal heat exchanger in South Korea. Sci. China Ser. E-Technol. Sci. 53, 123–128 (2010). https://doi.org/10.1007/s11431-009-0413-9

Li, H.F., Chen, M.Q., Fu, B.A., Liang, B.: Evaluation on the thermal and moisture diffusion behavior of sand/bentonite. Applied Thermal Engineering. 151, 55–65 (2019). https://doi.org/10.1016/j.applthermaleng.2019.01.100

Liu, H., Rodriguez-Dono, A., Zhang, J., Zhou, N., Wang, Y., Sun, Q., Zhang, L.: A new method for exploiting mine geothermal energy by using functional cemented paste backfill material for phase change heat storage: Design and experimental study. Journal of Energy Storage. 54, 105292 (2022). https://doi.org/10.1016/j.est.2022.105292

Mascarin, L., Garbin, E., Di Sipio, E., Dalla Santa, G., Bertermann, D., Artioli, G., Bernardi, A., Galgaro, A.: Selection of backfill grout for shallow geothermal systems: Materials investigation and thermo-physical analysis. Construction and Building Materials. 318, 125832 (2022). https://doi.org/10.1016/j.conbuildmat.2021.125832

Mendes, J.C., Barreto, R.R., Paula, A.C.B., Da Elói, F.P.F., Brigolini, G.J., Peixoto, R.A.F.: On the relationship between morphology and thermal conductivity of cement-based composites. Cement and Concrete Composites. 104, 103365 (2019). https://doi.org/10.1016/j.cemconcomp.2019.103365

Mettler Toledo: Thermal Analysis in Practice Tips and Hints, Introductory Handbook. (2016)

Park, M., Min, S., Lim, J., Choi, J.M., Choi, H.: Applicability of cement-based grout for ground heat exchanger considering heating-cooling cycles. Sci. China Technol. Sci. 54, 1661–1667 (2011). https://doi.org/10.1007/s11431-011-4388-y

Pascual-Muñoz, P., Indacoechea-Vega, I., Zamora-Barraza, D., Castro-Fresno, D.: Experimental analysis of enhanced cement-sand-based geothermal grouting materials. Construction and Building Materials. 185, 481–488 (2018). https://doi.org/10.1016/j.conbuildmat.2018.07.076

Riegger, M., Rolker, J., Steger, H., Stober, I., Haist, M., Eckhardt, J.-D., Schlager, P., Zemann, M., Zorn, R., Huttenloch, P.: Abschlussbericht zu dem Forschungsvorhaben EWS-tech: Weiterentwicklung der Erwärmesonden-Technologie. (2016)

Schutter, G., Taerwe, L.: Specific heat and thermal diffusivity of hardening concrete. Magazine of Concrete Research. (1995)

Shafigh, P., Asadi, I., Akhiani, A.R., Mahyuddin, N.B., Hashemi, M.: Thermal properties of cement mortar with different mix proportions. Mater. construcc. 70, 224 (2020). https://doi.org/10.3989/mc.2020.09219

Song, X., Zheng, R., Li, R., Li, G., Sun, B., Shi, Y., Wang, G., Zhou, S.: Study on thermal conductivity of cement with thermal conductive materials in geothermal well. Geothermics. 81, 1–11 (2019). https://doi.org/10.1016/j.geothermics.2019.04.001

Viccaro, M.: Doped bentonitic grouts for implementing performances of low-enthalpy geothermal systems. Geotherm Energy. 6, (2018). https://doi.org/10.1186/s40517-018-0090-7

Wang, S., Jian, L., Shu, Z., Chen, S., Chen, L.: A High Thermal Conductivity Cement for Geothermal Exploitation Application. Nat Resour Res. 29, 3675–3687 (2020). https://doi.org/10.1007/s11053-020-09694-4

Xu, Y., Chung, D.D.L.: Effect of sand addition on the specific heat and thermal conductivity of cement. Cement and Concrete Research. 30, 59–61 (2000). https://doi.org/10.1016/S0008-8846(99)00206-9

Yang, Y., Li, B., Che, L., Li, M., Luo, Y., Han, H.: Calculation model and influence factors of thermal conductivity of composite cement-based materials for geothermal well. Geotherm Energy. 12, 3 (2024). https://doi.org/10.1186/s40517-024-00282-w

Zhao, J., Huang, G., Guo, Y., Feng, Z., Gupta, R., Liu, W.V.: Development of a novel cement-based grout with enhanced thermal and sealing performance for borehole heat exchangers. Energy and Buildings. 302, 113754 (2024). https://doi.org/10.1016/j.enbuild.2023.113754

Zhou, Y., Zhang, Y., Xu, Y.: Influence of grout thermal properties on heat-transfer performance of ground source heat exchangers. Science and Technology for the Built Environment. 24, 461–469 (2018). https://doi.org/10.1080/23744731.2017.1402645